12th Asia-Pacific Conference on Combustion,
Fukuoka International Congress Center, Fukuoka, Japan
1st -5th July 2019.

Auto-ignition in turbulent combustion of hydrogen/air mixing layer at high pressure

Wenhao Yang[1], Tong Yao[1], Yiran Chen[1], Kai Hong Luo[2]

[1]Center for Combustion Energy, Key Laboratory for Thermal Science and Power Engineering of Ministry of Education,
Department of Energy and Power Engineering, Tsinghua University
Beijing 100084, China

[2]Department of Mechanical Engineering, University College London
Torrington Place, London WC1E 7JE, UK

Abstract

The present work investigates the dynamic process of auto-ignition and extinction of flame kernels in a hydrogen/air mixing layer at a pressure of 30 atm. Direct numerical simulation (DNS) is conducted to solve the unsteady compressible flow equations coupled with reduced chemistry and detailed transport. The evolution of ignition kernels is tracked and analysed, focusing on the differences between successful and failed kernels. Parameters such as the temperature, heat release rate, scalar dissipation rate, convective and diffusive heat fluxes are calculated to provide quantitative information about ignition kernel development. The convective and diffusive heat fluxes in the successful and failed cases show marked differences. Finally, chemical explosive mode analysis (CEMA) is conducted to provide additional information.

Keywords: Partially premixed combustion; Hydrogen/Air combustion; Auto-ignition and extinction; Chemical explosive mode analysis; Direct Numerical Simulation (DNS);

1 Introduction

Hydrogen is now used as fuel or fuel addictive in practical engines like HCCI and gas turbine combustors [2,3]. With three distinct kinetic regimes, the ignition process of hydrogen has been studied in homogeneous and non-homogenous, laminar and turbulent configurations. To investigate the features of the hydrogen ignition process in detail, Direct Numerical Simulations (DNS) is widely used by researchers. Pantano [4] and Hawkes et al [5] employ DNS to show that extinction and reignition are prevalent in the turbulent jet diffusion flames. Mastorakos et al [6,7] shows that auto-ignition in a mixing layer between a hot oxidizer and a cold fuel in a turbulent flow always occurs at the most reactive mixture fraction, along which the scalar dissipation rate has low values. Meanwhile, the time evolution of the volume average conditional scalar dissipation rate $< \chi \mid f_{MR} >$ until autoignition shows that small ignition delay time occurs always when $< \chi \mid f_{MR} >$ is low. Echekki et al [8] investigates the evolution of different kernels in hydrogen/air auto-ignition, which emphasizes the instantaneous balance between radical production and dissipation. The effective Damköhler number must remain above a certain value in the process of auto-ignition. Venugopal et al [9] investigates the features of extinction and reignition dynamics in non-premixed flame-vortex interactions in laminar non-premixed flames. The effects of convective and diffusive heat fluxes in the flames are discussed. Im et al [10] use DNS to study the features of auto-ignition in hydrogen/air with an isotropic homogeneous decaying turbulence. Detailed chemical kinetics are employed and the simulated pressure is 1 atm. In addition, the effects of diffusion are investigated by Hilbert and Thévenin [11], the Lewis number being unity in the study. Yao et al. [12] have studied the auto-ignition features of hydrogen/air mixing layer at elevated pressures, which shows the importance of H_2O_2 and HO_2 as radical sinks during the ignition process. Besides, OH radicals can be used as a marker for the transition of auto-ignition to flame propagation.

The objective of the present study is to gain further insight into the auto-ignition process at a high pressure, including the roles of heat convection and diffusion. As a computational diagnostic method, the chemical explosive mode analysis (CEMA) [13] is employed to identify the detailed flame structure. It is shown that CEMA is a critical feature in ignition as well as extinction regions, which can be utilized as a marker of explosive or pre-ignition mixtures.

2 Method

2.1 Numerical methods

The DNS code PARCOMB [14] solves the fully compressible Navier-Stokes equations. A sixth-order central scheme for space discretization and an explicit fourth-order Runge-Kutta time integrator are employed. The extended Navier-Stokes Characteristic Boundary Conditions (NSCBC) [15,16] are usedto implement non-reflecting boundary conditions and pressure relaxation is applied along all open faces. The code utilizes a reduced chemical scheme of 9 species (H_2, O_2, H_2O, OH, H, O, HO_2, H_2O_2, and N_2) and 37 reactions [17] to describe the combustion of hydrogen in air, considering the effects of multicomponent diffusion velocities and thermo-diffusion.

Mixture fraction ξ characterizes the level of mixing between the reactants. It takes a value of 0 in pure oxidizer and a value of 1 in pure fuel. The following formulation is used in the present work,

$$\xi = \frac{(Y_H - Y_{H,ox}) / 2W_H - (Y_O - Y_{H,ox}) / 2W_O}{(Y_{H,fu} - Y_{H,ox}) / 2W_H - (Y_{O,fu} - Y_{O,ox}) / 2W_O} \quad (1)$$

where Y_H and Y_O are the elemental mass fractions of elements H and O, and the subscript ox and fu state the oxidizer and fuel sides, respectively. W_H and W_O state the relative elemental masses for H and O, respectively. The scalar dissipation rate is computed by the expression

$$\chi = 2\alpha \nabla \xi \cdot \nabla \xi \tag{2}$$

where α is the thermal diffusivity.

2.2 Computational configuration

The computational domain is two-dimensional with periodic and subsonic non-reflecting boundary conditions. The domain size is 1cm×1cm. On the right side, we set initial temperature T=300K, mass fraction of oxygen Y_{O2}=0.233, mass fraction of hydrogen Y_{H2}=0, and mass fraction of nitrogen Y_{N2}=0.767. On the left side, we set initial temperature T=1100K, mass fraction of hydrogen Y_{H2}=0.023, mass fraction of oxygen Y_{O2}=0, and mass fraction of nitrogen Y_{N2}=0.977. The initial velocities are set equal to zero. The initial temperature and mixture fraction are shown in Fig. 1. The mixing layer between fuel and air is specified as the hyperbolic-tangent profiles with a stiffness parameter s=2000. The initial mixture fraction is set by the following expression in the full domain

$$\xi = \frac{1}{2}[1 - \tanh(s - (x - x_m))] \tag{3}$$

where x_m is the middle of the x coordinate.

Turbulent conditions are illustrated as follows. The turbulent rms fluctuation u'=0.29m/s, the integral length scale l_t=0.29mm, the turbulent time scale $\tau_t = 1.0ms$, and the turbulent Reynolds number Re_t=148 describe the turbulence. The Kolmogorov scale $l_K = 7\mu m$ is calculated to determine the spatial resolution and a 5001×5001 grid is used in the computational domain. The Kolmogorov scales are resolved by 3~4 grid points which are tested to be adequate. The time step is controlled by the CFL number.

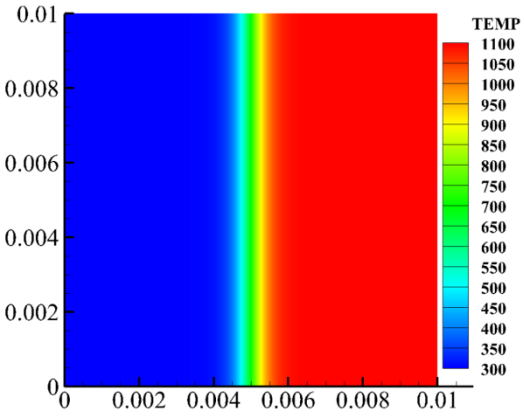

Figure 1: Initial temperature conditions

3 Results and Discussions

In order to study the influence of high pressure on the auto-ignition and extinction of hydrogen/air turbulent combustion, the pressure is set to 30atm in the present study. The total physical time simulated is 5.5ms, costing 49.8 hours using xxx compute cores. The first auto-ignition kernel appears at $\tau_{idt} = 3.433ms$ in this case.

3.1 Flame development

Figures 2a-2d shows the sequence of ignition kernel development in terms of temperature. The stoichiometric mixture fraction contour lines, Z_{sto}=0.56, and most reactive fraction, Z_{mr}=0.05, are overlaid on the temperature contours in the figures. As the fuel interacts with the oxidizer strongly under the influence of turbulence, the mixing layer shows wrinkling and large curvature. Subsequently, auto-ignition occurs on the fuel-lean side, along the most reactive mixture fraction iso-line. HO_2 and H_2O_2 can be used as a good marker variable for identification of ignition spots.

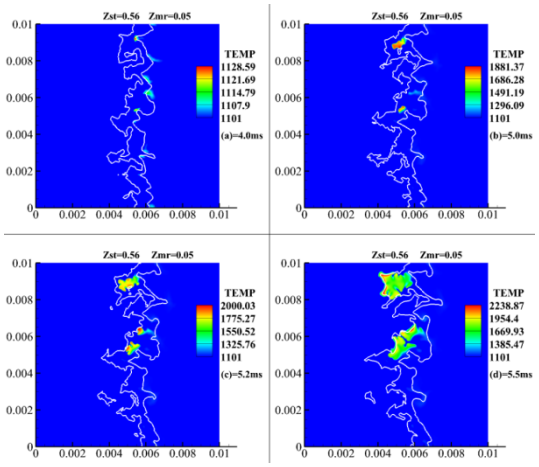

Figure 2: Ignition temporal development

The temperatures at auto-ignition positions are high, whereas local scalar dissipation rates are low, which can be seen in Fig. 3. High scalar dissipation rate causes heat loss from the auto-ignition kernels. The overlapping region in Fig. 3 demonstrates that the wrinkled interface of mixing layer. The kernels grow and move from the most reactive mixture fraction toward the stoichiometric mixture fraction. It is seen from Fig. 2c and Fig. 2d that the kernels then evolve along the stoichiometric mixture fraction iso-line, and form stable and very thin flame fronts (Fig. 2d). In addition, we also observe the interactions between flame fronts.

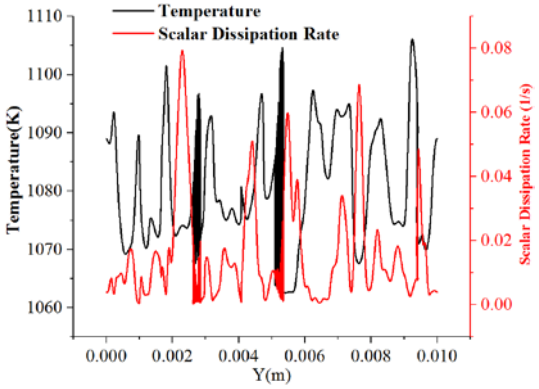

Fig. 3: Temperature and scalar dissipation rate profile as a function of Y axis along the most reactive mixture.

3.2 Auto-ignition and extinction kernels

There are about five auto-ignition kernels initially. However, only three of them sustain and form stable flame fronts. We will now focus on the evolution of auto-ignition and extinction of four kernels in the mixing layer, as shown in the Fig. 4. We will examine four parameters: temperature, heat release rate, convective and diffusive heat fluxes computed by the following expressions

$$CX = \rho u \frac{\partial h}{\partial x}$$

$$CY = \rho v \frac{\partial h}{\partial y}$$

$$DX = \frac{\partial}{\partial x}\left(\frac{\lambda}{c_p}\frac{\partial h}{\partial x}\right)$$

$$DY = \frac{\partial}{\partial y}\left(\frac{\lambda}{c_p}\frac{\partial h}{\partial y}\right) \quad (4)$$

where CX and CY are the convection terms for the mixture-specific enthalpy h in the X and Y directions, respectively; DX and DY are the diffusion terms for h in the X and Y directions, respectively, and ρ , u, v, λ and c_p are the mixture density, X-velocity, Y-velocity, mixture thermal conductivity, and mixture specific heat.

Figures 5a-5d show the evolution of temperature and heat releaser rate for the four kernels. There is an obvious difference between kernels A, B, C and E. In Figs. 5a-5c, the heat release rate increases sharply over a very short period of time while the temperature keeps increasing. In contrast, the heat release rate and temperature first increase slowly and then decrease together, for kernel E in Fig. 5d. Besides, the peak values of the heat release rate for the successful ignition kernels are about one order of magnitude higher than the failed kernel.

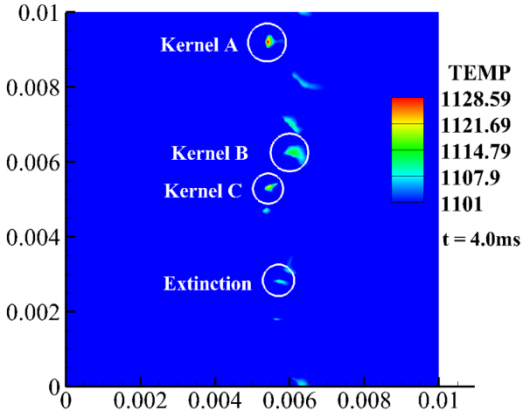

Figure 4: Research Kernels

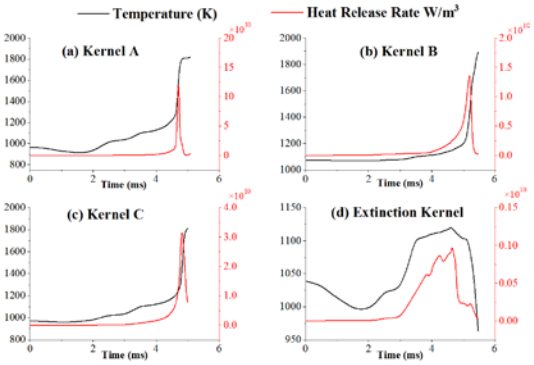

Figure 5: Evolution of temperature and heat release rate

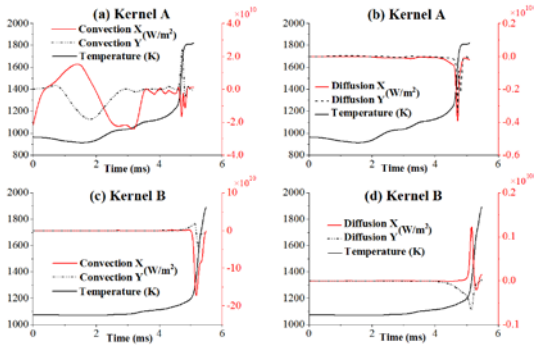

Figure 6: Evolution of temperature and convective and diffusive heat fluxes in Kernel A and B

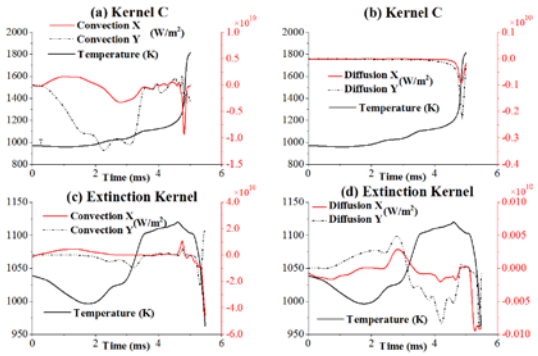

Figure 7: Evolution of temperature and convective and diffusive heat fluxes in Kernel C and D

Figures 6a-6d and Figures 7a-7d show the evolution of temperature and convection heat fluxes, diffusion heat fluxes in X, Y directions, respectively. Both convection and diffusion terms undergo a huge undulation as the temperature increases. However, the final state reveals that these two terms are approaching zero for mature auto-ignition kernels. In contrast, in the failed kernel, the two terms in the Y direction go up sharly and in the X direction go down. These findings demonstrate that the balance among the convective and diffusive heat fluxes is important to the sustainability of ignition kernels.

3.3 Chemical Explosion Mode Analysis of kernels

The auto-ignition kernels are examined using the chemical explosion mode analysis (CEMA), developed as a diagnostic technique to delineate explosive regions from normal flames. In this paper, we calculate the eigenvalue of the Jacobian matrix of the chemical source terms in the species and temperature equations, which play critical roles in explosive chemical processes and in demarcating the pre- and post-ignition mixtures in auto-ignition and flames. Figure 8 shows the temporal development of the eigenvalue (lamda) of the auto-ignition process in the mixing layer. By definition, the eigenvalues greater than zero indicate pre-ignition mixture and lower than zero indicate ignited mixture. Therefore, while red denotes a highly explosive mixture, blue denotes a highly reactive near-equilibrium mixture. However, no regions including the extinction kernels can be found in CEMA temporal development, even if there is the temperature rise in related regions.

Compared with temperature temporal development (Fig. 3), the chemical explosive regions are relatively small. And it is not easy to differentiate the details of flame features in Figure 8 because the eigenvalues are too small. Partially premixed flame

fronts are indicated by showing the abrupt transition between the pre-ignition (red) and post-ignition (blue) mixtures in Fig. 8.

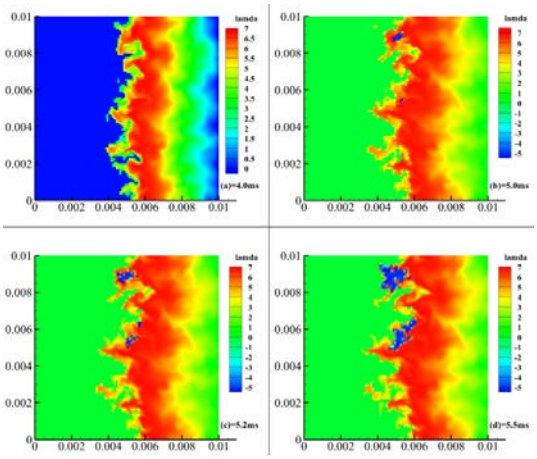

Figure 8: Temporal development of eigenvalues of chemical explosive mode analysis temporal development

4 Conclusions

In this paper, we investigated the dynamic process of auto-ignition and extinction in the mixing layer of hydrogen/air through two-dimensional DNS under a high pressure of 30 atm. In agreement with previous findings, the ignition kernels start at the most reactive mixture fraction, grow and the move toward the stoichiometric mixture iso-line, where kernels form stable flame fronts. Moreover, for the successful auto-ignition kernels, the convective and diffusive heat fluxes, must reduce to zero during the process. Besides, high heat release rate is needed, accompanied by rapid increase of temperature. For the extinction kernels, the convective and diffusive terms fluctuate significantly throughout the process. The chemical explosive mode analysis is employed in the analysis, but is not able to predict the ignition kernels. It may be more accurate to identify the partially premixed flame fronts by means of CEMA.

5 Acknowledgment

Support from the Natural Science Foundation of China (Grant No. 91441120) and the Centre for Combustion Energy at Tsinghua University is gratefully acknowledged. The simulations were performed on ARCHER funded under the EPSRC project “UK Consortium on Mesoscale Engineering Sciences (UKCOMES)” (Grant No. EP/R029598/1).

References

[1] N. Perters, Turbulent Combustion, Cambridge University Press, 2000, p. 237.
[2] O. Stenlåås, M. Christensen, R. Egnell, B. Johansson, F.Mauss, Sae Fuels & Lubricants Meeting Exhibition. 6 (2011) 1481-1489
[3] S. Wang, C. Ji, B. Zhang, X. Liu, Int J Hydrogen Energy. 39 (2014) 7428–7436.
[4] C. Pantano, J. Fluid Mech. 514 (2004) 231–270.
[5] E.R. Hawkes, R. Sankaran, J.C. Sutherland, J.H. Chen, Proc. Combust. Inst. 31 (2007) 1633–1640.
[6] E. Mastorakos, T.A. Baritaud, T.J. Poinsot, Combustion and Flame 109 (1997) 198–223.
[7] E. Mastorakos, Progress in Energy and Combustion Science 35 (2009) 57-97.
[8] T. Echekki, J.H. Chen, Combustion and Flame 134 (2003) 169–191.
[9] R. Venugopal, Combustion and Flame 153 (2008) 442-464.
[10] H.G. Im, J.H. Chen, C.K. Law, Twenty-Seventh Symposium (International) on Combustion, The Combustion Institute, Pittsburgh, 1998, p. 1047.
[11] R. Hilbert, D. Thévenin, Combustion and Flame 138 (2004) 175-187.
[12] T. Yao, W. Yang, K. H. Luo, Comput and Fluids 173 (2018) 59-72.
[13] Z. Luo, C. Yoo, E.S. Richardson, J.H. Chen, C.K. Law, T. Lu, Combustion and Flame 159 (2012) 265-274.
[14] D. Thévenin, F. Behrendt, U. Mass, B. Przywara, J. Warnatz, Comput Fluids 25 (1996) 485-496.
[15] M. Baum, T. Poinsot, D. Thévenin, J. Comput. Phys. 116 (1995) 247–261.
[16] T. Poinsot, S. Lele, J. Comput. Phys. 101 (1992) 104–129.
[17] U. Maas, J. Warnatz, Combustion and Flame 74 (1989) 475-488.